Contents lists available at ScienceDirect

Carbon Trends

Methodology for the identification of carbonyl absorption maxima of carbon surface oxides in DRIFT spectra

Felix Herold[a], Oliver Leubner[a], Katharina Jeschonek[a], Christian Hess[b], Alfons Drochner[a], Wei Qi[c], Bastian J.M. Etzold[a,*]

[a] *Department of Chemistry, Technical University of Darmstadt, Ernst-Berl-Institut für Technische und Makromolekulare Chemie, 64287 Darmstadt, Germany*
[b] *Department of Chemistry, Technical University of Darmstadt, Eduard-Zintl-Institut für Anorganische und Physikalische Chemie, 64287 Darmstadt, Germany*
[c] *Shenyang National Laboratory for Materials Science, Institute of Metal Research, Chinese Academy of Sciences, Shenyang 110016, China*

ARTICLE INFO

ABSTRACT

Carbon surface oxides have been demonstrated to be crucial for high performing carbon materials in various applications. Diffuse reflectance infrared Fourier transform spectroscopy represents a powerful time-resolved method to study the surfaces of functional materials under process conditions. Due to the severe overlap of the contributions of individual surface groups in combination with compared to organic molecules shifted absorption maxima meaningful analysis remains challenging. Especially due to the unknown maxima, deconvolution of the superimposed bands is strongly hindered. In this study, we developed a procedure based on hydrolysis, thermal annealing or a combination thereof, which allows to disentangle carbonyl absorption maxima of carboxylic acids, anhydrides and lactones on carbon surfaces. In order to verify the proposed transformations, thorough characterization by temperature programmed desorption, X-ray photoelectron spectroscopy, potentiometric titration and Boehm titration was carried out. Applying this procedure for a polymer derived reference material, the carbonyl absorption maximum could be deduced, which are positioned for lactones at 1771 cm^{-1}, for carboxylic acids between 1753 cm^{-1} and 1760 cm^{-1}, and for carboxylic anhydrides at 1792 cm^{-1} and 1852 cm^{-1}. This allowed deconvolution of the carbonyl band, paving the way for *in situ* time-resolved analyses.

1. Introduction

In light of the current efforts to reduce anthropogenic influences on the environment, carbon materials represent key-components of several technical applications. Due to a unique set of properties, combining high chemical stability with large surface areas, tunable porosity and a rich surface chemistry, carbon is the material-of-choice in various processes[1]. For instance, functional carbon materials are an important class of adsorbents utilized in waste water purification [2,3], gas storage [4–6] and gas separation [3,7]. In addition, carbon materials are used in energy storage [8–10] and to a considerable extent in catalysis [11,12] (*e.g.* as catalyst or support in water splitting [13,14], fuel cells [15–17] hydrogenations [18], dehydrogenations [19,20], hydroformylation [21]). Since all the mentioned applications rely on interactions between the carbon surface and a second gaseous or liquid phase, in addition to

carbon texture, the surface chemistry plays a crucial role. By creating a tailored ensemble of oxygen surface groups, carbon materials can be optimized for specific applications. In waste water purification, carbon surface oxides can be used to enhance the sorption capacity of polar adsorbates and further to enable selective adsorption in multicomponent mixtures [22,23]. Similarly, tailored surface oxide ensembles can be used to increase the capacitance of supercapacitors [24,25], performance of batteries [10], to increase dispersion [26,27] and control the size [26] of active metal catalysts and can finally act as catalytic centers themselves [28–31].

Carbon surface oxide ensembles are not rigid systems, meaning that changes in overall concentration and composition may occur upon changing environment. In this context, parameters such as temperature and chemical environment (*e. g.* pH; electrical potential, O_2, H_2) induce an adaptation of surface oxide ensembles by desorption, oxidation, reduction, condensation and hydrolysis. In this case, a viable option to gain reliable information of the carbon surface chemistry under process conditions are *in situ* analysis techniques. However, measured by the high technical relevance

* Corresponding author.
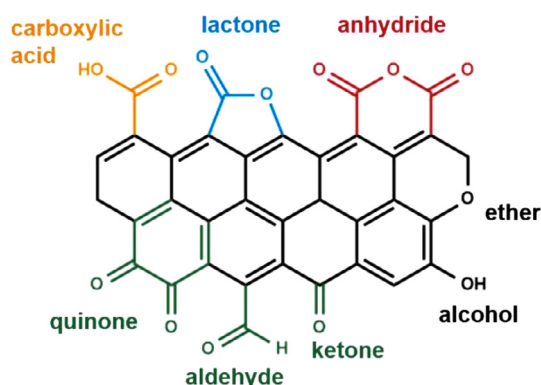 *E-mail address:* bastian.etzold@tu-darmstadt.de (B.J.M. Etzold).

Fig. 1. Model of abundant surface oxides on carbon surfaces.

of the surface chemistry of sp^2 hybridized, porous carbon materials, such as activated carbon and carbon black, possibilities for *in situ* analysis are significantly underdeveloped. In this sense, *in situ* analyses of carbon surface oxides have so far only been applied sporadically, for example in the investigation of carbon-based dehydrogenation catalysts, whereas *in situ* titration and near ambient pressure X-ray photoelectron spectroscopy (XPS) were used[30,31]. While *in situ* titration (selective poisoning of active centers) is a powerful strategy to quantify active sites and deduce reaction pathways, it is based on chemical modification of the carbon surface and yields information on only one individual surface species. Near ambient pressure XPS can provide a large amount of useful information, whereas this method is limited to reactant pressures of a few millibars. Among other methods, diffuse reflectance infrared Fourier transform spectroscopy (DRIFT spectroscopy) appears to be especially suitable for the *in situ* analysis of oxygen surface groups on carbon, as it offers the advantage of being able to operate at process conditions in terms of pressure, temperature as well as atmosphere, and the measurement itself does not influence the sample composition.

Meldrum et al. used *in situ* DRIFT spectroscopy to examine the influence of several gaseous reactants (*e.g.* O$_2$, CO$_2$, H$_2$O, NH$_3$) at various temperatures on surface oxides on technically relevant sp^2 hybridized carbon [32,33]. Upon contact with oxidants (O$_2$, CO$_2$) at elevated temperatures, DRIFT spectroscopy enabled to observe the oxidation of an activated carbon, indicated by developing absorption of C=O double and C−O single bonds. Introduction of nucleophiles such as H$_2$O and NH$_3$ lead to shifting changes in carbonyl absorption, assigned to the hydrolysis of carboxylic anhydrides.

However, despite the high sensitivity of spectral features such as the carbonyl band to changes in the composition of the surface oxide ensemble, interpretation of IR spectra provides a major challenge due to severe overlap of the contributions of individual surface groups to the νC=O absorption region (1600 – 1900 cm^{-1}) and, even more pronounced, to the νC-O, δ_O-H and δ_C-H absorption range (1500 – 1000 cm^{-1}). Considering the carbonyl absorption as spectral feature least affected by overlap, this absorption band is a superposition (in case of the simplified model molecule (Fig. 1)) of contributions of carboxylic acids, lactones, anhydrides and carbonyl species represented by ketones, aldehydes and quinones. In principle, meaningful quantitative information can be extracted from IR bands that represent a superposition by mathematical deconvolution, but in this case the absorption maxima of the individual contributions must be known.

In this context, carboxylic acids have been assigned to wavenumbers ranging from 1700 - 1765 cm^{-1}, whereas most studies suggest absorption maxima in proximity to 1720 cm^{-1} [32,34–40]. Carbonyl absorption of carboxylic acids is heavily influenced by the presence or absence of hydrogen bonds, meaning that the

maxima of the νC=O band in carboxylic acid dimers (connected by two hydrogen bonds (eg. 1709 cm^{-1} for the benzoic acid dimer)) can be shifted to lower wavenumbers by up to 40 cm^{-1} compared to the carbonyl absorption of the corresponding monomer (1752 cm^{-1} for the benzoic acid monomer) [41]. In this sense, as carboxylic acid dimers should be quite rare on carbon surfaces, the "true" absorption maximum (in absence of water) is probably found towards the higher-wavenumber end of the absorption range considered in literature. The carbonyl absorption maximum of lactones has been assigned to wavenumbers ranging from 1710 to 1790 cm^{-1} whereas some studies seem to agree on the assignment of the νC=O vibration of lactones to 1740 cm^{-1} [34,35,37–39,42,43]. Anhydrides are localized in general at higher wavenumbers, contributing two absorption bands to the carbonyl absorption of oxygen functionalized carbons, separated by approximately 60 cm^{-1}. The lower wavenumber maximum is located in the region between 1750 – 1790 cm^{-1} while the higher wavenumber absorption is assigned to a range between 1830 and 1900 cm^{-1} [32,33,35,38,44,45]. Finally, the νC=O of ketones on carbon surfaces has been assigned to the absorption range between 1660 – 1720 cm^{-1} [36,37,43,46,47] while the absorption maximum of the carbonyl band of aldehydes has been located at 1720 cm^{-1} [36,38] and that of quinones in the range of 1655 - 1690 cm^{-1} [43,46]. Other studies localize the νC=O vibration of unspecified carbonyl species conjugated to the carbon backbone in the region between 1600 - 1710 cm^{-1} [32,33,35,45].

The dissonance with regard to the assignment of absorption maxima in the carbonyl region (1600–1900 cm^{-1}) of IR spectra reflects on one hand the diverse chemical environments of the individual surface oxides, introduced by the reaction of various oxidants (e. g. O$_2$ [44], CO$_2$ [33], HNO$_3$ [36], H$_2$O$_2$ [39]) on different carbon backbones (*e.g.* activated carbon [43], carbon black [44], carbon nanotubes [46]). On the other hand, studies often go without the additional application of complementary analytical methods such as Boehm titration, temperature programmed desorption (TPD) or XPS, turning the interpretation of IR spectra into a major challenge due to the complexity of carbon surface oxide ensembles.

Since a prominent influence of the carbon backbone on the absorption maxima of individual surface oxides is highly plausible, the corresponding absorption maxima would have to be determined for each new material. In this context, a simple procedure for a reliable identification of these properties would represent a significant advance.

In this work, we present strategies to derive the νC=O absorption maxima in IR spectra of carboxylic acids, lactones and anhydrides on carbon surfaces based on simple wet-chemistry hydrolysis of carboxylic acid derivatives and heat treatment procedures, or a combination thereof (Fig. 2). As reference material, a polymer derived carbon was utilized, which offered similar properties to technically important amorphous porous carbons, but at a higher chemical purity and especially reproducibility[48]. The proposed transformations of carbon surface oxide ensembles are closely evaluated by a comprehensive analytical approach, including DRIFT spectroscopy, titration methods, TPD and XPS and allowed to determine the carbonyl absorption (νC=O) of lactones, carboxylic acids and carboxylic anhydrides.

2. Materials and methods

2.1. Materials

All gases were purchased from Westfalen AG. Phloroglucinol and methanol were purchased from Acros Organics. Pluronic F127 and 37 wt-% formaldehyde solution were supplied by Sigma Aldrich. From Fisher Scientific, 37 wt-% hydrochloric acid, techni-
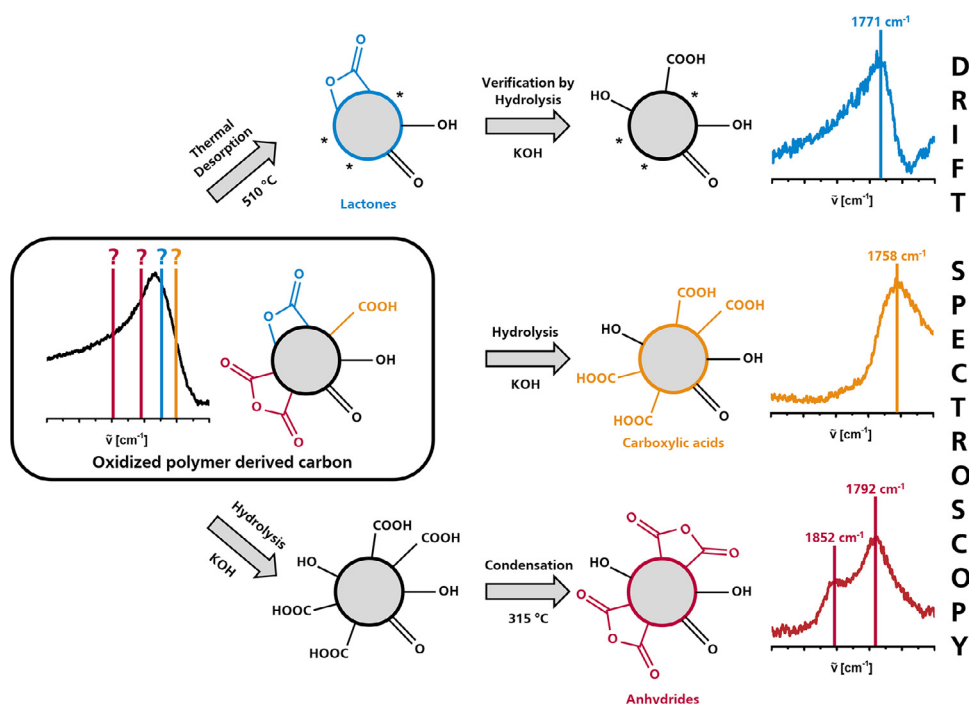
Fig. 2. General procedures for obtaining selectively functionalized carbon materials by hydrolysis and heat treatment procedures, in order to identify carbonyl absorption maxima for lactones, carboxylic acids and anhydrides.

cal grade ethanol and 65 wt-% nitric acid purchased. Alfa Aesar supplied potassium nitrate. Potassium hydroxide (85 wt-%) as well as calibration buffers for the potentiometric titration and Boehm titration were purchased from Carl Roth. Standard solutions for potentiometric and Boehm titration (0.1 M HCl, 0.01 M HCl, 0.1 M KOH, 0.01 M KOH, 0.01 N Na_2CO_3, 0.01 N $NaHCO_3$) were purchased from Merck.

2.2. Carbon precursor

To obtain the carbon precursor, a synthesis procedure following Herold et al. was applied [48]. In short, in a 3 L round bottom flask, 26.2 g Phloroglucinol (1,3,5-trihydroxy benzene), 52.4 g Pluronic® F127 and 10 g 37 wt-% HCl are heated under stirring with a KPG stirrer (500 rpm, half-moon impeller, 70 mm blade) in 1320 mL EtOH to reflux. Upon addition of 26 g 37 wt-% aqueous Formaldehyde solution, the reaction mixture turns turbid within minutes. After refluxing for 2 h, a yellow precipitate is collected by filtration. After washing thoroughly with EtOH and vacuum drying at 30 mbar and 60 °C, 47.3 g of bright yellow polymer aggregates are obtained.

2.3. Pyrolysis

20 g of polymer particles are subjected to pyrolysis in a horizontal tubular furnace (Carbolite Gero GmbH) under a flow of 20 dm³ h⁻¹ (STP) He. The samples are heated at a rate of 120 °C h⁻¹ from room temperature to 850 °C, this temperature level is maintained for 2 h, subsequently the samples are cooled to room temperature with a cooling rate of 120 °C h⁻¹. After cooling, 8 g of polymer-derived carbon are obtained.

2.4. Hydrothermal NOₓ oxidation

In a PTFE coated autoclave (Berghof Products + Instruments, DB-500) 5.0 g of carbon are suspended in 250 mL of 1,5 M aqueous HNO_3. The autoclave is heated with a heating jacket adjusted to 180 °C. As soon as the internal temperature reaches a point 15 °C below the adjusted external temperature (165 °C), the "reaction timing" starts. After 1 h, the autoclave is transferred to a water bath (RT) to cool. After cooling, reaction gases (NO_x, CO_2) are released by a needle valve and passed through diluted aqueous KOH. The resulting oxidized carbon is collected by filtration, washed thoroughly with deionized water and is dried at 60 °C and 30 mbar. After drying, 3.73 g of oxidized polymer-derived carbon (abbreviated as O-PDC) are obtained.

2.5. Thermal annealing

In a STA 409 PC Luxx thermogravimetry device (NETZSCH GmbH), 200 mg of carbon are heated under a flow of 30 mL/min (STP) He in a Al_2O_3 crucible with a rate of 5 K/min to the desired temperature. The target temperature is maintained for 1 h, subsequently the sample is cooled to room temperature with a cooling rate of 10 K/min.

The use of thermal treatments is indicated in the name of samples when using *HeXXX°C*, where *He* marks heat treatment in helium atmosphere while *XXX* refers to the employed temperature (for example O-PDC-He510 °C).

2.6. Hydrolysis with KOH

In a round-bottom flask equipped with a cooler, 500 mg of O-PDC are suspended in 100 mL 3 M aq. KOH. The oil bath is heated to the desired temperature, and is stirred with a magnetic stirrer for the desired time. Upon cooling, the liquid is removed by centrifugation/decantation and the carbon sample is re-suspended for 2 h in 100 mL 10 wt-% aq. HCl in order to neutralize residual/adsorbed KOH. Afterwards, the carbon sample is collected by centrifugation and washed thoroughly with a H_2O/MeOH mixture (approx. 4:1 vol:vol) and is dried at 60 °C and 30 mbar.
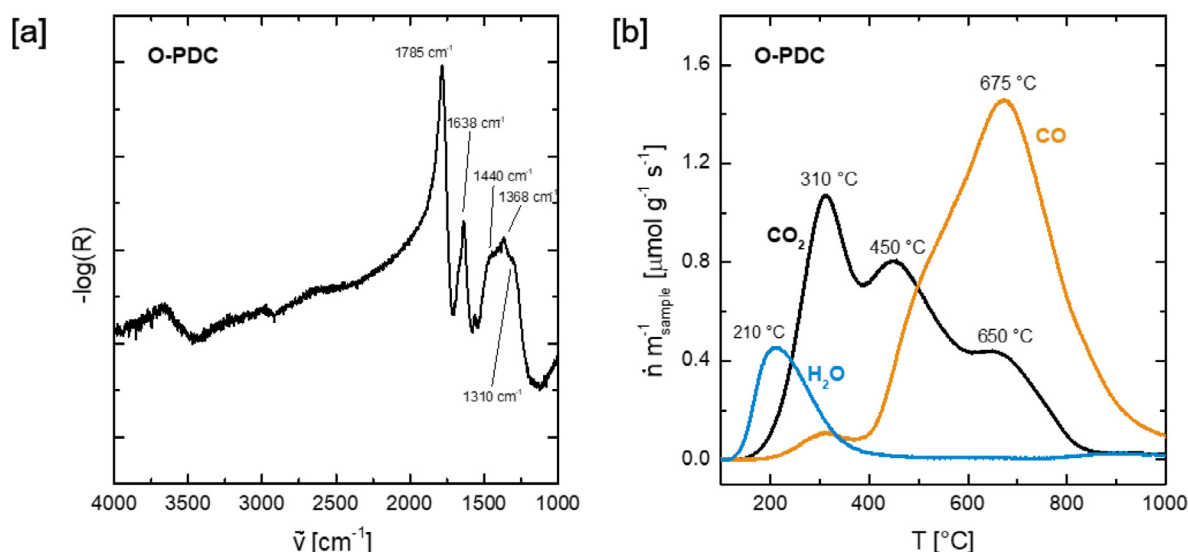
Fig. 3. [a] DRIFT spectrum of oxidized polymer-derived carbon. [b] TPD of oxidized polymer-derived carbon.

The use of KOH hydrolysis is indicated in the name of samples by using annotations following the logic of *KOH-temperature-reaction time* (for example O-PDC-KOH-RT-24 h).

For obtaining O-PDC-He510 °C-KOH, a suspension of O-PDC-He510 °C is stirred in 3 M KOH for 72 h at an oil bath temperature of 120 °C. O-PDC-KOH refers to O-PDC treated with 3 M KOH at 60 °C for 24 h (*e. g.* O-PDC-KOH-60 °C-24 h).

2.7. Reproducibility

All experiments were carried out at least twice, whereas no problems with reproducibility were encountered.

2.8. Analytics

DRIFT spectroscopy was conducted employing a Bruker VERTEX 70 spectrometer with a Praying Mantis diffuse reflection accessory (Harrick Scientific) at a resolution of 1 cm^{-1}, using KBr as a reference. TPD measurements were carried out in a STA 409 PC Luxx thermogravimetric balance (NETZSCH) coupled to a calibrated on-line mass spectrometer (Omnistar, Pfeiffer Vacuum) at a heating ramp of 5 °C min min^{-1} with He as carrier gas. Deconvolution of TPD emission profiles was conducted using a procedure proposed by Pereira, Figueiredo and co-workers [49–51]. XPS was carried out using a SSX 100 ESCA spectrometer (Surface Science Laboratories) employing monochromatic Al Kα irradiation. Potentiometric titration was conducted on an automatic titrator T50 (Mettler Toledo) from pH 3 to pH 11, dosing a constant amount of 0.1 M KOH every 1200s. Proton sorption isotherms and the corresponding acidity constant distributions were derived from potentiometric titration curves according to a procedure proposed by Bandosz and co-workers [52]. Boehm titration was executed according to a procedure published by Ackermann et al. by contacting the carbon samples with 0.01 N solutions of NaHCO$_3$, Na$_2$CO$_3$ and NaOH for 48 h, followed by acidification with 0.01 N HCl and titration with 0.01 N Na$_2$CO$_3$[53]. Elemental analysis was carried out using a Vario EL III (Elementar Analysesysteme) device employing O$_2$ as oxidant and a gas chromatograph for the quantification of gasification products.

For detailed analytic procedures concerning TPD, potentiometric titration, Boehm titration, DRIFTS, XPS and elemental analysis see the supporting information.

3. Results and discussion

3.1. Oxidized polymer derived carbon as base material for this study

Base material for the study is a recently introduced reference material for amorphous porous carbons using polymer derived carbon which is NO$_x$ oxidized under hydrothermal conditions (1.5 M HNO$_3$, 180 °C, denoted as oxidized polymer derived carbon (O-PDC)). Characterization of the pristine polymer derived carbon is described in detail elsewhere [48]. The hydrothermal treatment with HNO$_3$ introduces a high oxygen loading of 34.3 wt-% (Table S1).

DRIFT spectroscopy of O-PDC reveals two distinct absorption bands centered at 1785 cm^{-1} and 1638 cm^{-1} with a local minimum at 1705 cm^{-1}, corresponding to νC=O vibrations and to the absorption of substituted C=C moieties and surface carbonates [44]. The third observable signal is a rather broad absorption centered at 1368 cm^{-1} with shoulders at 1440 cm^{-1} and 1310 cm^{-1}, representing contributions of νC-O and δ_O-H vibrations. The position of the maximum of the νC=O vibration in the DRIFT spectrum of O-PDC indicates the presence of carboxylic acid derivatives, especially carboxylic anhydrides (Fig. 3a).

TPD of O-PDC shows distinct CO$_2$ evolution maxima at 310, 450 and 650 °C, corresponding to the desorption of carboxylic acids, carboxylic anhydrides and lactones (Fig. 3b) [50,54–57]. CO evolution is detected in a temperature range from 400 °C to 1000 °C, with the maximum located at 675 °C. This broad signal is most likely a superposition of the CO evolution in consequence of the decomposition of alcohols, carbonyl species (aldehydes, ketones, quinones) and ethers (Table S2) [50,54–57]. Besides CO and CO$_2$, also a significant amount of chemisorbed water is detected between 150 and 400 °C, speaking for the occurrence of thermal induced condensation reactions.

Potentiometric titration with KOH of O-PDC revealed a significant ion exchange capacity of 3.81 mmol g^{-1}, suggesting the presence of a significant concentration of acidic surface oxides on O-PDC (Figure S1a). This could be verified by Boehm titration of O-PDC, whereas 2.73 mmol g^{-1} NaHCO$_3$, 3.20 mmol g^{-1} Na$_2$CO$_3$ and 4.02 mmol g^{-1} NaOH were consumed (Figure S1b). In this context, the comparatively high NaHCO$_3$ uptake indicates a high concentration of carboxylic acids on the surface of O-PDC.

XPS of O-PDC underscores these findings, with carbon species amounting to 82.1 at-% of the overall surface composition, with
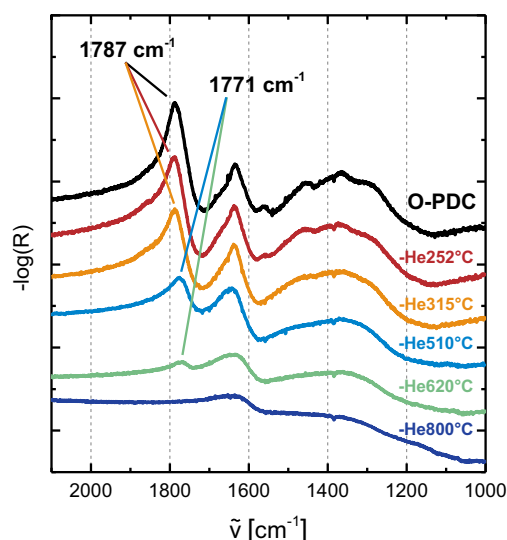
Fig. 4. DRIFT spectra of O-PDC and O-PDC after thermal annealing in inert atmosphere at various temperatures.

61.8 at-% of the surface atom ensemble represented by carbon species exclusively bound to carbon, 9.2 at-% by carbon species bound by a single bond to oxygen (C–O), 3.1 at-% by carbonyl species (C=O) and 8.1 at-% by carbon in carboxylic acid and its derivates (O-C=O, Table S3 and Figures S2-S4). Oxygen surface species amount to 17.9 at-% of the overall surface composition, with 5.4 at-% present as carbonyl oxygen species (found in anhydrides, lactones, aldehydes, ketones and quinones), 6.2 at-% as oxygen in carboxylic acids and 5.8 at-% corresponding to oxygen in ethers and alcohols (with the balance being physically adsorbed water, Figures S3 and S4, Table S4).

In summary, the harsh hydrothermal oxidation yields a carbon material with high oxygen loading present in form of a wide variety of different carbon surface oxides, that resembles hydrothermally oxidized carbons discussed in literature [58,59] and is well-represented by the model "molecule" shown in Fig. 1.

3.2. Identification of lactone IR-bands through carbon materials submitted to thermal desorption

To study the carbonyl absorption of lactones, the high thermal stability of lactones compared to carboxylic acids and anhydrides was exploited in order to "isolate" lactones by removing acids and anhydrides via thermal desorption at 510 °C while lactones remain on the carbon surface. Following this approach, additional to lactones also aldehydes, ketones and quinones can attribute to the νC=O absorption, as they exhibit high desorption temperatures well over 700 °C [48,50,55–57,60]. However, on one hand, for the thermally annealed sample the concentration of these carbonyl species detected by analysis of the XPS C1s region is quite low (3.3 at-%, (Table S4)). On the other hand, the proposed absorption maxima of these groups (1655 cm^{-1} - 1720 cm^{-1}, see introduction) coincide directly with the observed local absorption minimum in the DRIFT spectrum of O-PDC centered at 1705 cm^{-1} (Fig. 3a), suggesting that the influence (meaning the extinction coefficient) of aldehydes, ketones and quinones on the νC=O contribution is rather low in general.

Fig. 4 shows DRIFT spectra of oxidized carbons which were thermally annealed between 252 °C and 800 °C (the chosen temperatures were inspired by DÜNGEN et al. [55]; for a TPD analysis of the annealed carbons see Figure S5). Upon heating O-PDC to

510 °C, a shift in the position of the carbonyl absorption was detected (by 16 cm^{-1} from 1787 cm^{-1} to 1771 cm^{-1}, Figs. 4 and 5b) and thermal treatment of O-PDC in inert gas at 510 °C (denoted as O-PDC-He510 °C) was subsequently employed further for deriving the carbonyl absorption of lactones (Fig. 5a). It should be noted at this point, that the desorption temperature range of anhydrides and lactones overlaps to some extent (see Table S2), meaning that quantitative desorption of anhydrides simultaneously results in the removal of temperature labile lactones.

Upon heating O-PDC to 510 °C in inert atmosphere, the oxygen content drops significantly from 34.3 wt-% for O-PDC to 16.5 wt-% for O-PDC-He510 °C, indicating the loss of a significant fraction of the surface oxide ensemble (Table S1).

TPD of O-PDC-He510 °C reveals that the annealing procedure does not exhibit a pronounced influence on the emitted amount of CO (+ 2%), however the CO emission profile is narrowed and a significant higher CO evolution can be detected in the region of the desorption maximum around 680 °C (Fig. 5c). The amount of desorbed CO_2 decreases by 66%, while the amount of chemisorbed water, released between 150 °C and 500 °C, decreases by 87%. The CO_2 desorption is detected as a single desorption peak centered at 665 °C, which falls in the desorption temperature range of lactones proposed in the literature (Fig. 5c, Table S2) [50,54–57]. It should be noted at this point, that re-oxidation of defects caused by anhydride and carboxylic acid desorption upon exposure to air does not seem to play a substantial role, as no significant CO_2 evolution below the annealing temperature of 510 °C could be observed during TPD. The fitting of TPD CO and CO_2 emission profiles building on a procedure proposed in the literature verifies the observed changes (Figures S6 and S7) [49–51].

This result is mirrored by Boehm titration, whereas the base consumption drops upon thermal annealing for NaHCO$_3$ by 90% from 2.73 to 0.27 mmol g^{-1}, for Na$_2$CO$_3$ by 90% from 3.20 mmol g^{-1} for O-PDC to 0.32 mmol g^{-1} for O-PDC-He510 °C and in case of NaOH by 91% from 4.02 to 0.36 mmol g^{-1} (Fig. 5d). The loss of strongly acidic surface groups (*e. g.* carboxylic acids and anhydrides) is further verified by potentiometric titration, as the ion exchange capacity drops sharply by 81% from 3.81 mmol g^{-1} to 0.71 mmol g^{-1} (Figure S8). Extraction of the acidity constant distribution from the potentiometric titration curves shows that contributions assigned to carboxylic acids of O-PDC (at pKa 3.1 and 5.7) decline substantially upon thermal annealing of O-PDC (Figure S9).

Analysis of the O1s XPS contribution of O-PDC-He510 °C shows in general a decrease of the concentration of oxygen surface species (−28%), whereas the decrease in carboxylic acid surface concentration is disproportionate high (C=O species decrease by 15%, C-O-R by 14%, COOH decreases by 48%)(Figures S3 and S4, Table S3, for detailed analysis of the C1s contribution, see Table S4 and Figures S3 and S4). In this context, the applied fitting model for the O1s XPS region yields a sharp rise in the ratio of C=O/COOH species (C=O corresponds to lactones, anhydrides, aldehydes, ketones and quinones; COOH corresponds to carboxylic acids) from 0.87 for O-PDC to 1.46 for O-PDC-He510 °C.

In order to verify if the identity of the isolated, CO_2-emitting groups as lactones, KOH hydrolysis was employed, to convert surface lactones into carboxylic acids and the corresponding hydroxyl groups (Fig. 5a). Upon contact with KOH, the oxygen content increased from 16.5 wt-% for O-PDC-He510 °C to 21.2 wt-% for O-PDC-He510 °C-KOH, indicating a significant uptake of OH$^-$ ions (Table S1). In the DRIFT spectrum, the KOH hydrolysis leads to a further shift in the νC=O contribution from 1771 to 1753 cm^{-1}, indicating that the dominant species in the spectrum is indeed sensitive to OH$^-$ (Fig. 5b).

TPD of O-PDC-He510 °C-KOH reveals an increase of CO_2 emission by 16%, as in addition to the emission maximum centered at
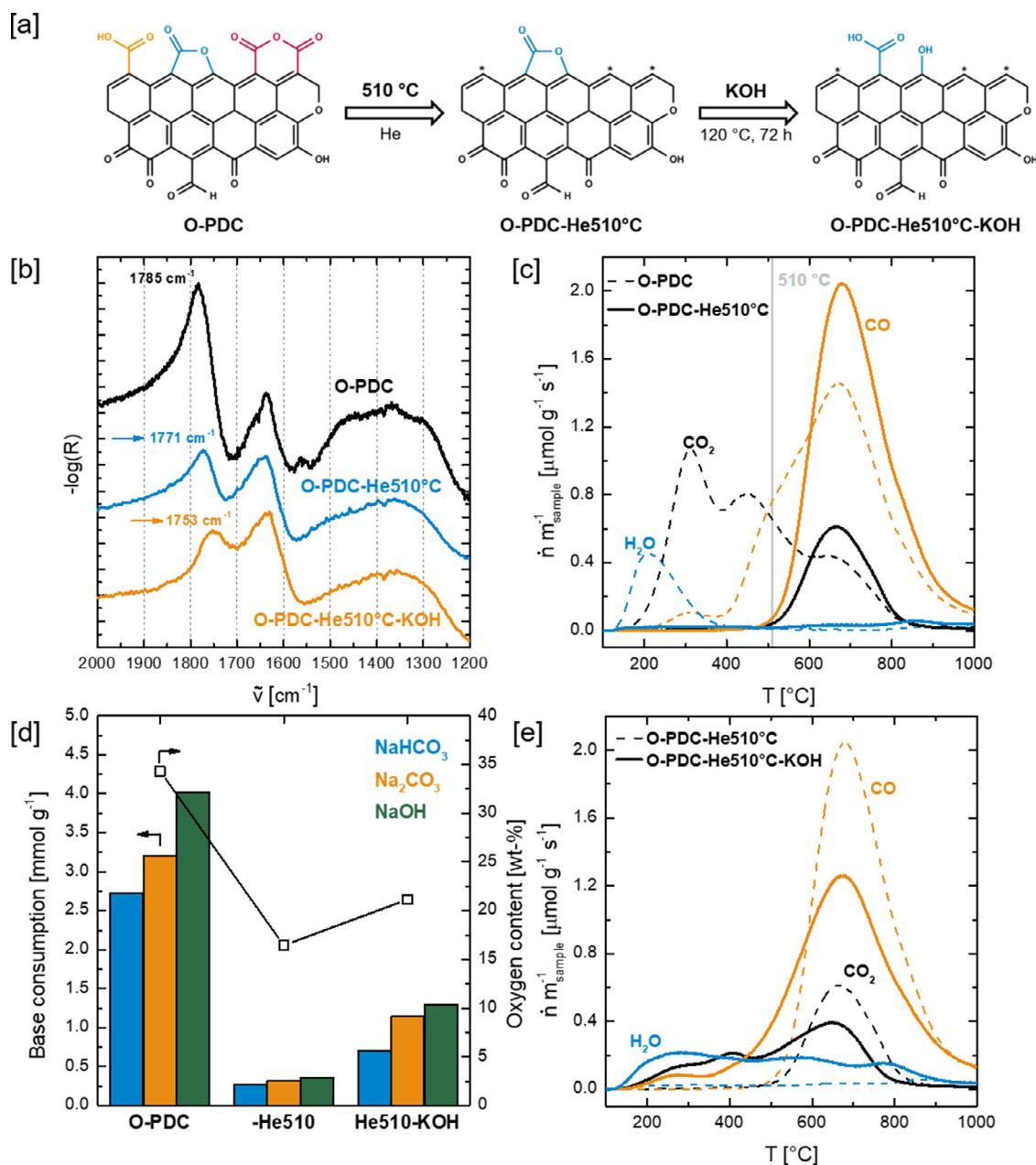
Fig. 5. [a] Synthetic procedure for the isolation of lactones by thermal annealing at 510 °C and verification by hydrolysis of the lactones with KOH. [b] DRIFT spectra of O-PDC, O-PDC-He510 °C and O-PDC-He510 °C-KOH. [c] Comparison of the TPD profiles of O-PDC and O-PDC-He510 °C. [d] Boehm titration and oxygen content (elemental analysis) of O-PDC, O-PDC-He510 °C and O-PDC-He510 °C-KOH. [e] Comparison of the TPD profiles of O-PDC-He510 °C and O-PDC-He510 °C-KOH.

650 °C observed with O-PDC-He510 °C, CO_2 emission at lower temperatures, with a maximum at 400 °C (corresponding to the desorption of anhydrides) and a shoulder at 300 °C (corresponding to carboxylic acid decomposition) reappears upon contact with KOH (Fig. 5e). The detection of the significant CO_2 emission at 650 °C and 400 °C which is attributed to the decomposition of lactones with O-PDC-He510 °C-KOH does not contradict the success of the hydrolysis reaction, as it yields neighboring hydroxyl groups and carboxylic acids which are prone to thermally induced condensation. These condensation reactions are important side reactions in TPD and are indicated by the significant emission of water in the case of O-PDC-He510 °C-KOH between 150 and 500 °C. In this sense, the lactones detected in the CO_2 emission profile of O-PDC-He510 °C are present in the pristine sample prior heat treatment during TPD analysis, as no significant evolution of water could be detected. In contrary, lactones and anhydrides observed in the CO_2

emission profile of O-PDC-He510 °C-KOH are likely to be a product of condensation reactions, as a significant amount of chemically adsorbed water could be detected during TPD. The TPD difference plot between O-PDC-He510 °C and O-PDC-He510 °C-KOH confirms the formation of carboxylic acid groups and anhydrides, showing maxima in relative CO_2 emission centered at 275 °C, 400 °C and 510 °C (Figure S10). A minimum in relative CO_2 emission is detected at 680 °C, indicating a decrease in concentration of surface lactones. The CO difference plot reveals a maximum in relative CO emission at 530 °C, and a minimum centered at 680 °C. The maximum in relative emission at 530 °C can be attributed to the desorption of hydroxyl groups, which are formed upon lactone hydrolysis [48]. This increase in carboxylic acids, anhydride and phenol concentration upon contact with KOH could also be verified by the fitting of the CO and CO_2 emission profiles (Figures S6 and S7).
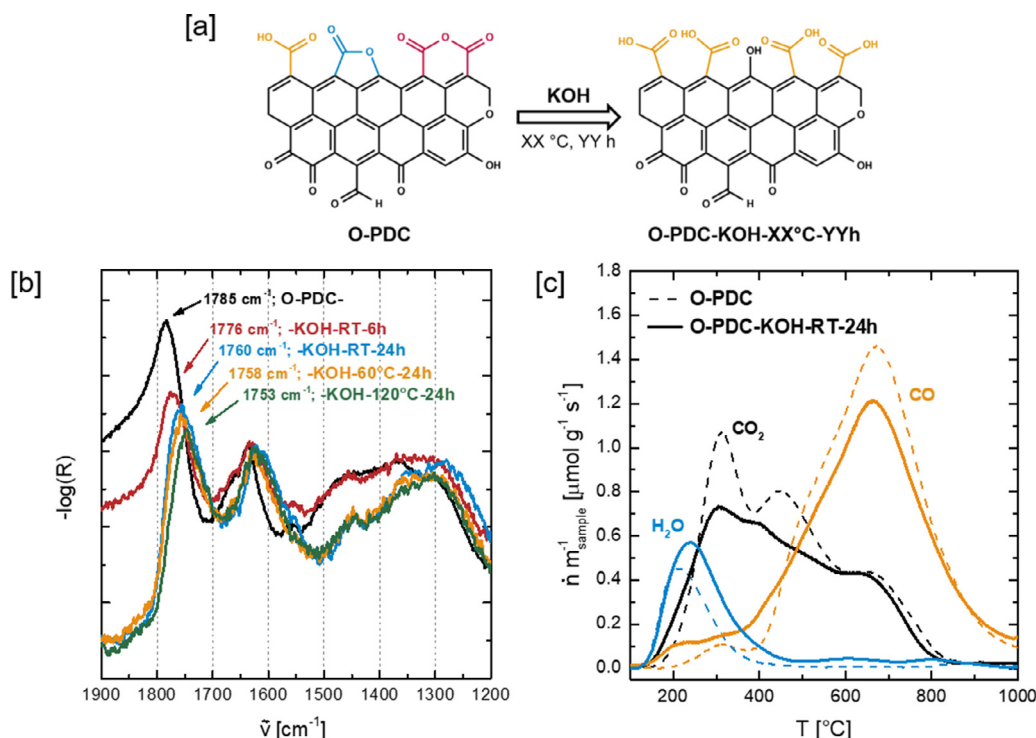
Fig. 6. [a] Synthetic procedure for hydrolysis of anhydrides and lactones to form carboxylic acids. [b] DRIFT spectra of O-PDC and O-PDC contacted with 3 M KOH at various conditions (-RT-6 h; RT-24 h; −60 °C-24 h; −120 °C-24 h). [c] Comparison of the TPD profiles of O-PDC and O-PDC-KOH-RT-24 h.

Especially Boehm titration draws a clear picture, with an increase in NaHCO$_3$ consumption of 163% from 0.27 mmol g^{-1} for O-PDC-He510 °C to 0.71 mmol g^{-1} for O-PDC-He510 °C-KOH, a rise in Na$_2$CO$_3$ uptake by 256% (from 0.32 to 1.14 mmol g^{-1}) and an increase of NaOH consumption by 261% from 0.36 mmol g^{-1} to 1.30 mmol g^{-1} (Fig. 5d). In addition to the generation of highly acidic groups, the increase in NaOH suggests also a rise in concentration of weakly acidic surface groups such as phenols. The generation of acidic surface groups by KOH hydrolysis is further verified by potentiometric titration, whereas the ion exchange capacity increases by 36% from 0.71 mmol g^{-1} to 0.97 mmol g^{-1} (Figure S8).

Analysis of the XPS O1s region of O-PDC-He510 °C-KOH shows a drop in the concentration of C=O species (-15%), while the surface concentration of -COOH rises by 100% (Figures S3 and S4, Table S3, for detailed analysis of the C1s contribution, see Table S4 and Figures S3 and S4). This change is reflected by the C=O/COOH ratio, which drops sharply upon contact to KOH from 1.46 for O-PDC-He510 °C to 0.61 for O-PDC-He510 °C-KOH.

In conclusion, the successful thermal desorption of carboxylic acids and anhydrides at 510 °C led to a carbon material enriched in lactones and from its DRIFT spectra it can be deduced that the lactone carbonyl absorption maximum is positioned at 1771 cm^{-1}. The following, generalized procedure can therefore be applied to any carbon material: Starting at 450 °C (desorption maximum of anhydrides), isothermal desorption is carried out with gradually increasing temperature until a shift of the DRIFTS carbonyl band occurs. The resulting position of the carbonyl absorption maximum of lactones can be verified by KOH hydrolysis and subsequent identification of hydroxyl and carboxylic acids as reaction products.

3.3. Identification of carboxylic acid IR-bands through carbon materials submitted to hydrolysis

As the cleavage of lactones to form carboxylic acids and hydroxyl groups appeared to be successful, this approach was transferred to O-PDC without the thermal annealing step, in order to obtain a carbon mostly occupied by carboxylic acids by hydrolysis of carboxylic anhydrides and lactones. For this purpose, O-PDC was treated with 3 M KOH. Using different contact times and temperatures, conditions for near quantitative conversions were deduced (Fig. 6a).

The base treatment leads to an initial loss of total oxygen detected by elemental analysis, which increases with rising treatment temperature and duration from 34.3 wt-% for O-PDC down to 27.3 wt-% for O-PDC-KOH-120 °C-24 h which is most likely caused by base catalyzed decarboxylation (Table S1) [61]. DRIFT spectroscopy shows a shift of the νC=O absorption band from 1785 cm^{-1} to 1776 cm^{-1} when O-PDC is contacted with KOH at room temperature for 6 h (Fig. 6b). Treatment with KOH for 24 h at room temperature leads to a more pronounced shift by 25 cm^{-1} from 1785 to 1760 cm^{-1}. At this point, the hydrolysis reaction appears to be close to completeness, as rising the temperature from room temperature to 60 °C does not yield a significantly changed νC=O shift (1758 cm^{-1}). Although the hydrolysis at 120 °C leads to a slight shift of the carbonyl band from 1785 to 1753 cm^{-1}, it is also associated with the greatest loss of total oxygen, with the harsh reaction conditions increasing the probability of decarboxylation reactions. These observations imply a successful hydrolysis of the lactones and anhydrides of O-PDC, since a wide range of increasingly harsh reaction conditions (room temperature → 120 °C) produce a similar shift of the carbonyl band (from 1785 cm^{-1} for O-PDC to 1760 – 1753 cm^{-1} for the KOH treated carbons) (Fig. 6b).

TPD profiles reflect the loss of total oxygen, as the amount of emitted oxygen (considering CO$_2$, CO and H$_2$O emission) decreases for all KOH treated samples (-RT-6 h −9%; -RT-24 h −8%; −60 °C-24 h −6%; 120 °C-24 h −27%) (Figs. 6c, S11). TPD profiles for O-PDC-KOH-RT-6 h, O-PDC-KOH-RT-24 h and O-PDC-KOH-60 °C-24 h exhibit similar shapes, characterized on one hand by insignificant changes in the CO desorption profile and consequently in the concentrations of CO emitting species determined by fitting the TPD CO emission profile (Figures S11 - S13). Paradoxically, KOH treatment of O-PDC leads to a decrease in CO$_2$ desorption in the range
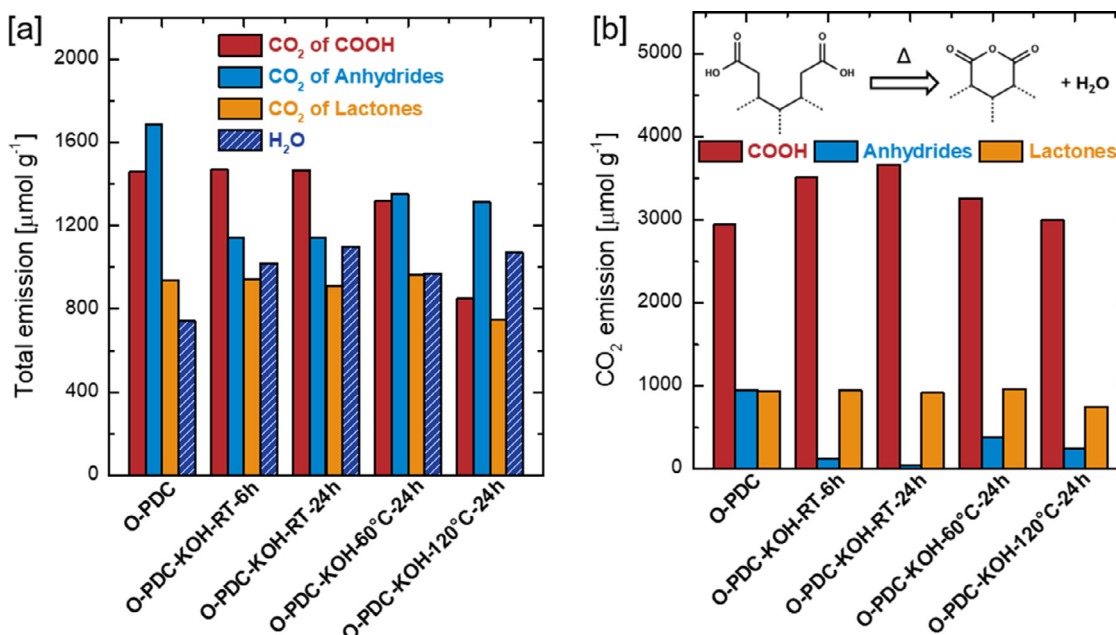
Fig. 7. [a] Total water emission and results of the fitting of the TPD CO_2 emission profile of O-PDC, O-PDC-KOH-RT-6 h, O-PDC-KOH-RT-24 h, O-PDC-KOH-60 °C-24 h and O-PDC-KOH-120 °C-24 h. [b] Total CO_2 emission assigned to carboxylic acids, anhydrides and lactones of O-PDC treated with KOH under various conditions, calculated under the assumption that the total H_2O emission is caused by condensation of carboxylic acids to anhydrides upon heating.

between 200 and 400 °C, suggesting a decrease in surface concentration of carboxylic acids (Figs. 6c and 7a; Figures S11 and S14). At the same time, CO_2 evolution in the range between 400 and 500 °C, associated with the desorption of anhydrides also decreases, while the amount of CO_2 emitted in the range between 600 and 800 °C (assigned to the decomposition of lactones) remains constant [56,62]. In case of O-PDC-KOH-120 °C-24 h, the CO_2 emission between 200 and 400 °C, associated with the decomposition of carboxylic acids, is decreased to a greater extent compared to the other KOH treated samples (Fig. 7a, Figure S10d). This observation could be explained by decarboxylation of carboxylic acids due to the harsh reaction conditions over 24 h. However, besides CO and CO_2, a significant increase in H_2O evolution compared to O-PDC can be observed during TPD of all KOH treated samples between 150 and 500 °C (Fig. 7a, Figure S11).

H_2O emission is associated with side reactions during TPD, namely condensation reactions of carboxylic acids (forming anhydrides) and of carboxylic acids with hydroxyl groups (forming lactones) [55]. In consequence, the carbon surface oxide ensemble is altered to a great extent by heating in inert atmosphere, in a sense that the actual surface concentration of carboxylic acids of O-PDC is significantly underestimated, while the concentration of anhydrides and lactones of O-PDC is overestimated. Hydrolysis of lactones and anhydrides by KOH treatment yields reactive groups in close proximity to each other, creating ideal starting conditions for condensation reactions during TPD. The increased occurrence of condensation reactions is reflected by a higher H_2O emission of the KOH-treated samples between 150 and 500 °C, which increases by up to 49% in case of O-PDC-KOH-RT-24 h compared to O-PDC. Assuming that the total water emission is caused by the condensation reaction of carboxylic acids to form anhydrides (thereby neglecting formation of lactones and ethers) and considering the stoichiometry of this reaction, the "real" concentration of CO_2 emitting groups (carboxylic acids, anhydrides and lactones) without the influence of condensation reactions can be calculated (Fig. 7b).

Taking water emission as a consequence of anhydride formation upon heating into account, carboxylic acids become the dominant species on the KOH treated carbons by far. The validity of

the presented assumption is affirmed by titration techniques, as the concentration of carboxylic acids derived by TPD without considering water emission accounted only to roughly 50% of $NaHCO_3$ consumption determined by Boehm titration and to about 40% of the ion exchange capacity determined by potentiometric titration (Fig. 8). However, if water emission as consequence of the transformation of carboxylic acids to anhydrides is included into the analysis, the consistency between the COOH and anhydride concentrations obtained by TPD and the corresponding consumptions of $NaHCO_3$ (assigned to the deprotonation of carboxylic acids) and Na_2CO_3 (assigned to the "deprotonation" of anhydrides) during Boehm titration increased considerably (Fig. 8a). A similar trend is observed for the comparison of the COOH concentrations obtained by TPD (considering condensation reactions) with the ion exchange capacities obtained by potentiometric titration (Fig. 8b).

In this context, Boehm titration shows that the KOH-treatment produces materials of comparable surface acidity (consumption of $NaHCO_3$ from 2.51 to 2.72 mmol g^{-1}; Na_2CO_3 from 3.11 to 3.20 mmol g^{-1}; NaOH from 3.88 to 4.02 mmol g^{-1}), which could be an indicator for an overlap of hydrolysis and decarboxylation reactions, or on the other hand could be a consequence of charge accumulation on the carbon particles (Figure S15a). Due to the high oxygen loading, increasing deprotonation could lead to a build-up of negative charges on the particle surface, which might prevent further neutralization of acidic surface groups at the given pH of the corresponding base solutions. Similarly, potentiometric titration shows ion exchange capacities for O-PDC, (3.81 mmol g^{-1}) O-PDC-KOH-RT-6 h, (4.25 mmol g^{-1}) O-PDC-KOH-RT-24 h, (3.28 mmol g^{-1}) O-PDC-KOH-60 °C-24 h, (3.36 mmol g^{-1}) as well as O-PDC-KOH-120 °C-24 h (3.31 mmol g^{-1}) that do not differ extensively (Figure S15b). However, closer analysis of potentiometric titration curves by extraction of acidity constant distributions reveals the presence of an additional carboxylic acid species with a pKa in the range between 6.4 and 6.9, which is not observed in the acidity constant distribution of O-PDC. This new contribution might be assigned to carboxylic acids produced by hydrolytic cleavage of lactones and anhydrides (Figure S16).
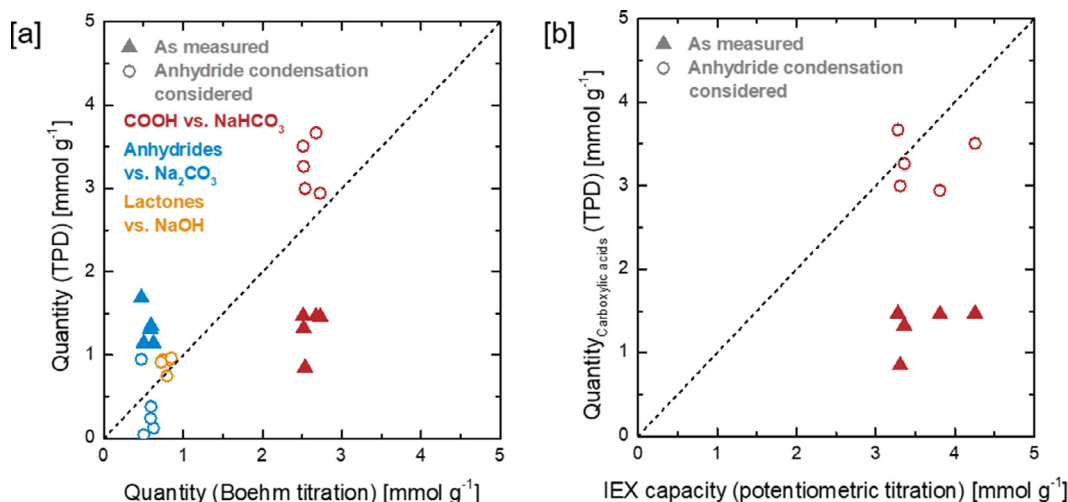
Fig. 8. [a] Correlation of the quantity of acidic surface groups obtained by fitting of the TPD CO_2 emission profile and Boehm titration. [b] Correlation of the quantity of carboxylic acids obtained by TPD fitting with the ion exchange capacity obtained by potentiometric titration. Full symbols display the quantification results as measured, while the empty symbols display the correlation when condensation of carboxylic acids to form anhydrides is taken into account.

Analysis of the XPS C1s region shows that the surface concentration of carbon bound to oxygen by single bounds (C-O 7.9 - 10.7 at-%),of carbonyl carbon species (2.8 - 3.7 at-%) and carbon bound in carboxylic acid derivatives (8.1 - 9.3 at-%) does not follow any trend upon KOH treatment, suggesting that the influence of side reactions might be low (Table S4, Figures S17 and S18). In case of the XPS O1s contribution, increasingly harsh KOH hydrolysis conditions lead to a decrease in concentration of the carbonyl oxygen contribution that is present in anhydrides, lactones, aldehydes, ketones and quinones (Table S3 and Figures S17 and S18). The surface concentration of carboxylic acids increases initially from 6.2 at-% of O-PDC to 8.1 at-% for O-PDC-KOH-RT-24 h and subsequently decreases to 6.3 at-% for O-PDC-KOH-60 °C-24 h and 6.1 at-% for O-PDC-KOH-120 °C-24 h. Overall, this results in a significant decrease in the C=O/COOH ratio, dropping from 0.87 for O-PDC to 0.31 for O-PDC-KOH-120 °C-24 h.

In conclusion, the results of the hydrolysis of O-PDC show some ambiguity due to overlapping influences of hydrolysis and decarboxylation. However, the good correlation of "condensation corrected TPD" with titration methods and, looking at the bigger picture, the successful hydrolysis of lactones as well as the successful re-condensation to anhydrides (see Section 3.4), strongly suggest that the proposed base hydrolysis procedure of lactones and anhydrides does indeed yield a carbon material largely occupied by carboxylic acids. Hence, the carbonyl absorption maximum of carboxylic acids can be assigned to a wavelength region between 1753 cm^{-1} and 1760 cm^{-1}. Again, this procedure can be applied for the identification of the position of the carbonyl absorption maximum of carboxylic acids for an arbitrary carbon material: For this purpose, hydrolysis with KOH is carried out with step wise increased contact times and reaction temperatures (under consideration of the wetting behavior). A convergence of the carbonyl absorption maximum upon increasingly harsh hydrolysis conditions indicates the position of the carbonyl absorption maximum of carboxylic acids.

3.4. Identification of carboxylic anhydride IR-bands through carbon materials submitted to a combination of hydrolysis and thermal desorption

Inspired by the observation of significant side reactions occurring during TPD analysis of KOH-treated O-PDC samples, these condensation reactions of carboxylic acids were exploited in an at-

tempt to produce a carbon surface largely occupied by carboxylic anhydrides. In this sense, O-PDC was first treated with KOH in order to create a high surface concentration of carboxylic acids, which were subsequently subjected to condensation by heating the carbon to 315 °C. This temperature was chosen as a compromise to induce the formation of carboxylic anhydrides by condensation of carboxylic acids and the quantitative desorption of unreacted carboxylic acids, while simultaneously preserving newly-formed anhydrides from decarboxylation. For the condensation reaction, O-PDC-KOH-60 °C-24 h (abbreviated in this chapter as O-PDC-KOH) was employed as starting material (Fig. 9a).

The overall oxygen content decreased initially from 34.3 wt-% for O-PDC to 30.3 wt-% for O-PDC-KOH and further after heat treatment at 315 °C to 23.6 wt-% for O-PDC-KOH-He315 °C (Table S1). DRIFT spectroscopy shows an initial shift of the $\nu C=O$ vibration maximum to lower wavenumbers from 1785 cm^{-1} for O-PDC down to 1758 cm^{-1} for O-PDC-KOH (Fig. 9b). By heat treatment at 315 °C, this shift is completely reversed, as the carbonyl band is shifted by 34 cm^{-1} from 1758 cm^{-1} to 1792 cm^{-1}. Additionally, a prior unobserved contribution emerges at 1852 cm^{-1} as a clear sign of the presence of cyclic anhydrides, which are usually characterized by two absorption maxima in the carbonyl region, separated by 50–60 cm^{-1} [32,38].

TPD shows a 25% decrease in CO_2 emission and a 12% increase in CO evolution for O-PDC-KOH-He315 °C compared to O-PDC-KOH (Fig. 9c). The TPD CO_2 emission profile indicates the absence of carboxylic acids, as no significant CO_2 evolution takes place below 300 °C and H_2O emission as a sign of side reaction also remains comparatively low. Two emission maxima can be observed, one between 400 and 500 °C that can be assigned to the decomposition of anhydrides and another centered at 650 °C that is associated with the desorption of lactones. These observations are further confirmed by the fitting of the TPD emission profiles (Figures S19 and S20). With the chosen procedure lactone formation can of course not be excluded, as re-condensation of neighboring carboxylic acids and hydroxyl groups cannot be prevented. In consequence of the influence of lactone carbonyl absorption, the "real" carbonyl absorption maximum of anhydrides will be slightly shifted to higher wavenumbers compared to experimentally extracted value. However, as the contribution of isolated lactones to the IR carbonyl absorption is already known (as discussed in Section 3.2), this does not limit the general approach.
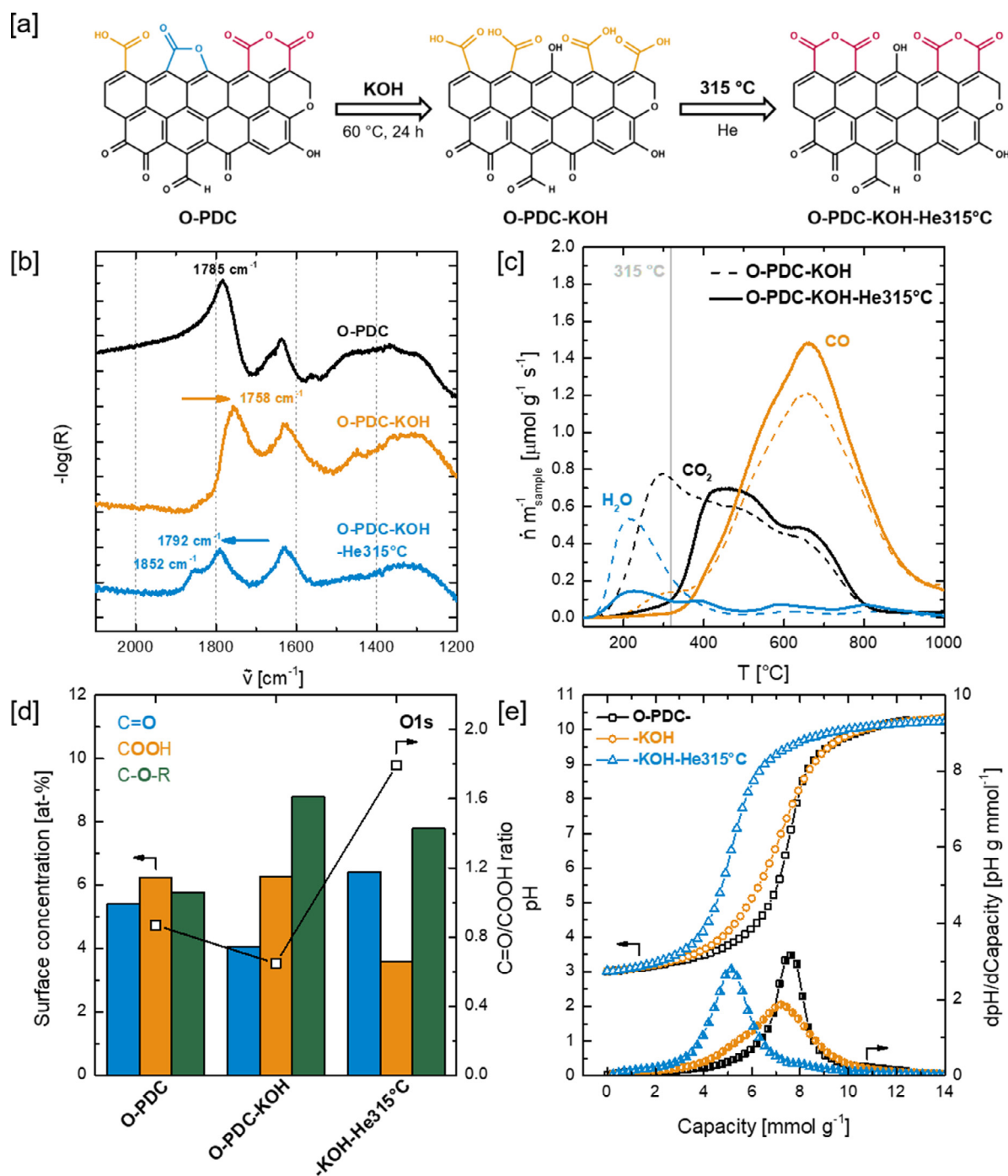
Fig. 9. [a] Synthetic procedure for the condensation of carboxylic acids in order to form carboxylic anhydrides. [b] DRIFT spectra of O-PDC, O-PDC-KOH and O-PDC-KOH-He315 °C. [c] Comparison of the TPD profiles of O-PDC-KOH and O-PDC-KOH-He315 °C. [d] Composition of oxygen species derived by analysis of the XPS O1s region of O-PDC, O-PDC-KOH and O-PDC-KOH-He315 °C. [e] Potentiometric titration of O-PDC, O-PDC-KOH and O-PDC-KOH-He315 °C.

Analysis of the XPS O1s region reveals that the surface concentration of carbonyl oxygen species (found in lactones, anhydrides, aldehydes, ketones and quinones) initially decreases by KOH treatment from 5.4 at-% for O-PDC to 4.1 at-% for O-PDC-KOH, whereas the heat treatment at 315 °C reverses this trend, increasing C=O surface concentration to 6.4 at-% (Figs. 9d, S21 Table S3 (For detailed analysis of the C1s contribution, see Figures S21 and S22, Table S4)). While the surface concentration of COOH does not change by treating O-PDC with KOH (6.2 at-% for O-PDC and 6.3 at-% for O-PDC-KOH), it decreases significantly upon thermal annealing at 315 °C (3.6 at-% for O-PDC-KOH-He315 °C). These results lead to

an initially decrease of the C=O/COOH ratio from 0.87 for O-PDC to 0.65 for O-PDC-KOH and subsequently to a considerable increase to 1.79 for O-PDC-KOH-He315 °C.

Potentiometric titration initially yields a slight decrease in ion exchange capacity from 3.81 mmol g^{-1} for O-PDC to 3.36 mmol g^{-1} for O-PDC-KOH, while heat treatment at 315 °C causes a decrease in ion exchange capacity down to 1.40 mmol g^{-1} for O-PDC-KOH-He315 °C, reflecting the loss of carboxylic acid groups (Fig. 9e). Regarding the acidity constant distributions, the two contributions of O-PDC (pKa 3.1 and 5.7) that can be assigned to carboxylic acids are initially joined by third one (pKa 6.6) in
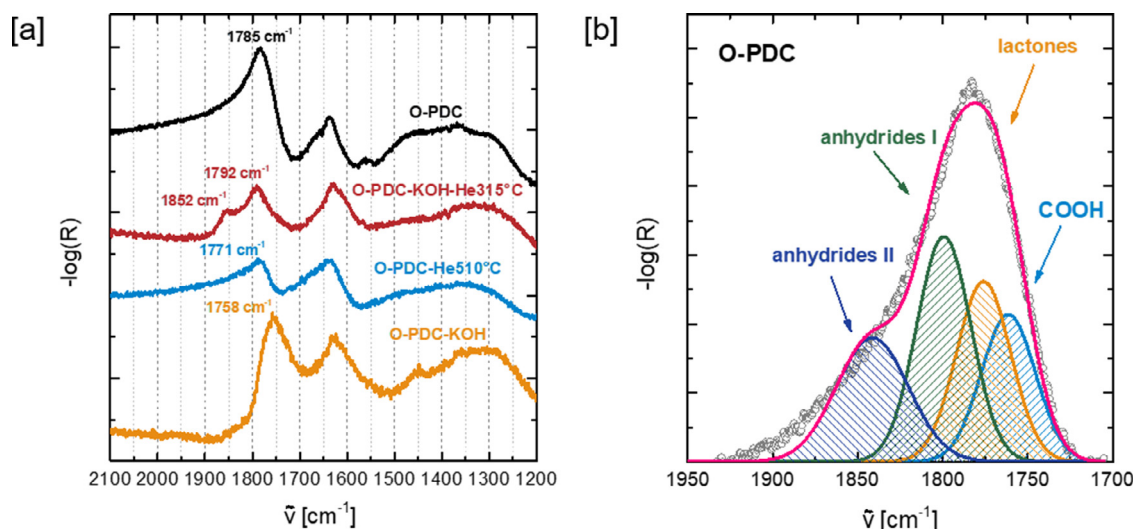
Fig. 10. [a] Comparison of DRIFT spectra of O-PDC, O-PDC-KOH, O-PDC-He510 °C and O-PDC-KOH-He315 °C. [b] Deconvolution of the carbonyl band of O-PDC, using the carbonyl absorption maxima derived in this work. Deconvolution was carried out by a least squares fit assuming contributions of individual surface oxides can be approximated with Gaussian profiles (for the method of baseline correction, see Figure S25).

case of O-PDC-KOH. However, in consequence of heat treatment at 315 °C, a substantial decline in all contributions assigned to carboxylic acids can be observed (Figure S23).

Boehm titration also shows an overall loss of acidic surface groups as consumption of NaHCO$_3$ drops from 2.52 mmol g^{-1} for O-PDC-KOH to 1.80 mmol g^{-1} for O-PDC-KOH-He315 °C, Na$_2$CO$_3$ decreases from 3.11 to 2.54 mmol g^{-1}, while NaOH uptake falls from 3.96 to 3.26 mmol g^{-1} (Figure S24). In case of Boehm titration, the differences between O-PDC-KOH and O-PDC-KOH-He315 °C are smaller than those observed with potentiometric titration, which might be explained by the difference in contact time. During Boehm titration, the carbon samples are contacted for 48 h with the corresponding base solutions, while potentiometric titration takes usually less than 20 h, with the average pH value being significantly lower. These circumstances lead in case of Boehm titration (deliberately) to cleavage and neutralization of carboxylic anhydrides, while this appears to be negligible during potentiometric titration. However, even the comparatively low pH value of 0.01 M NaHCO$_3$ solution appeared to induce a partial hydrolysis of anhydrides in case of O-PDC-KOH-He315 °C.

In conclusion, through hydrolysis of carboxylic acid derivates of O-PDC and subsequent thermal induced re-condensation, a carbon surface enriched in carboxylic anhydrides could be obtained and employed to extract the carbonyl absorption maxima of anhydrides at 1792 cm^{-1} and 1852 cm^{-1}. This method can be transferred to other carbon materials by first performing the hydrolysis discussed in chapter 3.3 to obtain a carbon material enriched with carboxyl groups. This material is then treated, starting at 300 °C, stepwise at higher temperatures until the carbonyl absorption maximum converges and both anhydride carbonyl contributions can be clearly identified in the DRIFT spectrum.

3.5. Combining data for the deconvolution of the drifts carbonyl band

The utilization of selective desorption, hydrolysis and (re-)condensation was found to be applicable to manipulate carbon surface oxides in general and to be suitable to transform carboxylic acid derivates into each other specifically. As could be shown by thorough characterization, the proposed approaches worked well to extract the absorption maxima of lactones at 1771 cm^{-1}, carboxylic acids between 1760 and 1753 cm^{-1} and anhydrides at

1792 and 1852 cm^{-1} which fall within the absorption ranges suggested by the literature (1710 - 1790 cm^{-1} for lactones [34,35,37–39,42,43], 1700 – 1765 cm^{-1} for carboxylic acids [32,34–40] and 1750 −1790 cm^{-1} as well as 1830 - 1900 cm^{-1} for anhydrides [32,33,35,38,44,45]), but can provide a significantly higher accuracy for the studied carbon material considering the broad absorption ranges given by literature.

Finally, considering the absorption regions for carboxylic acids (1753 - 1760 cm^{-1}), carboxylic anhydrides (1792 cm^{-1} and 1852 cm^{-1}) and lactones (1771 cm^{-1}) that can be extracted from the presented experiments, it is possible to construct the maximum and shape of the DRIFTS νC=O absorption of O-PDC as a super position of the contributions of carboxylic acids, anhydrides and lactones (Fig. 10). It should be noted at this point that DRIFT spectroscopy can only provide a non-trivial correlation between band intensity and concentration of a given species, since band intensities may vary with particle size and sample preparation, among other things [63]. However, if the surface concentration of a given surface oxide on a carbon sample is known (*e. g.* determined by TPD, XPS), changes in the carbon surface oxide ensemble can be monitored time resolved, quantitatively, under process conditions, by simply correlating the DRIFTS band intensity at the start of the *in situ* experiment with the known surface concentration [35].

4. Conclusion

In conclusion, we proposed a general methodology based on hydrolysis, thermal annealing or a combination thereof for the extraction of absorption maxima of the IR carbonyl band of carbon surface carboxylic acids, anhydrides and lactones. Using the example of an HNO$_3$ oxidized, polymer derived carbon, it could be shown that carboxylic acids and anhydrides can be removed selectively by thermal annealing in order to isolate lactones, which were found to exhibit a νC=O absorption maximum at 1771 cm^{-1}. Hydrolysis of lactones and anhydrides on the surface yielded a polymer derived carbon occupied largely by carboxylic acids, displaying the carbonyl absorption maximum between 1753 cm^{-1} and 1760 cm^{-1}. Surface anhydrides were formed by controlled re-condensation of carboxylic acids on a base treated oxidized carbon, and were found to exhibit two contributions to the carbonyl absorption centered at 1792 cm^{-1} and 1852 cm^{-1}.

Declaration of Competing Interest

The authors declare that they have no known competing financial interests or personal relationships that could have appeared to influence the work reported in this paper.

Acknowledgment

Supplementary materials

Supplementary material associated with this article can be found, in the online version, at doi:10.1016/j.cartre.2020.100020.

References

[1] F. Rodriguez-Reinoso, The role of carbon materials in heterogeneous catalysis, Carbon 36 (1998) 159–175.

[2] S. Pollard, G.D. Fowler, C.J. Sollars, R. Perry, Low-cost adsorbents for waste and wastewater treatment, Sci. Total Environ. 116 (1992) 31–52.

[3] J.M.D. Tascón (Ed.), Novel Carbon Adsorbents, Elsevier, Amsterdam, 2012.

[4] S.-.H. Yeon, S. Osswald, Y. Gogotsi, J.P. Singer, J.M. Simmons, J.E. Fischer, et al., Enhanced methane storage of chemically and physically activated carbide-derived carbon, J. Power Sources 191 (2009) 560–567.

[5] M.E. Casco, M. Martínez-Escandell, E. Gadea-Ramos, K. Kaneko, J. Silvestre-Albero, F. Rodríguez-reinoso, High-Pressure Methane Storage in Porous Materials, Chem. Mater. 27 (2015) 959–964.

[6] K. Kaneko, F. Rodríguez-Reinoso (Eds.), Nanoporous Materials for Gas Storage, Springer, Singapore, 2019.

[7] A. Ismail, L. David, A review on the latest development of carbon membranes for gas separation, J. Membr. Sci. 193 (2001) 1–18.

[8] A.G. Pandolfo, A.F. Hollenkamp, Carbon properties and their role in supercapacitors, J. Power Sources 157 (2006) 11–27.

[9] K.J. Kim, Y.-.J. Kim, J.-.H. Kim, M.-.S. Park, The effects of surface modification on carbon felt electrodes for use in vanadium redox flow batteries, Mater. Chem. Phys. 131 (2011) 547–553.

[10] S.W. Lee, N. Yabuuchi, B.M. Gallant, S. Chen, B.-.S. Kim, P.T. Hammond, et al., High-power lithium batteries from functionalized carbon-nanotube electrodes, Nat. Nanotechnol. 5 (2010) 531–537.

[11] I.C. Gerber, P. Serp, A theory/experience description of support effects in carbon-supported catalysts, Chem. Rev. 120 (2020) 1250–1349.

[12] P. Serp, J.L. Figueiredo (Eds.), Carbon Materials For Catalysis, John Wiley & Sons, Hoboken, NJ, 2009.

[13] Y. Xu, M. Kraft, R. Xu, Metal-free carbonaceous electrocatalysts and photocatalysts for water splitting, Chem. Soc. Rev. 45 (2016) 3039–3052.

[14] Y. Ding, M. Greiner, R. Schlögl, S. Heumann, A metal free electrode, ChemSusChem (2020) 4064–4068.

[15] A.L. Dicks, The role of carbon in fuel cells, J. Power Sources 156 (2006) 128–141.

[16] X. Liu, L. Dai, Carbon-based metal-free catalysts, Nat. Rev. Mater. 1 (2016) 16064.

[17] B. Ladewig, S.P. Jiang, Y. Yan (Eds.), Materials For Low-Temperature Fuel Cells, Wiley-VCH, Weinheim, 2015.

[18] T. Fu, Z. Li, Review of recent development in Co-based catalysts supported on carbon materials for Fischer–Tropsch synthesis, Chem. Eng. Sci. 135 (2015) 3–20.

[19] J. Gläsel, J. Diao, Z. Feng, M. Hilgart, T. Wolker, D.S. Su, et al., Mesoporous and graphitic carbide-derived carbons as selective and stable catalysts for the dehydrogenation reaction, Chem. Mater. 27 (2015) 5719–5725.

[20] W. Qi, D. Su, Metal-free carbon catalysts for oxidative dehydrogenation reactions, ACS Catal 4 (2014) 3212–3218.

[21] A. Weiß, M. Munoz, A. Haas, F. Rietzler, H.-.P. Steinrück, M. Haumann, et al., Boosting the activity in supported ionic liquid-phase-catalyzed hydroformylation via surface functionalization of the carbon support, ACS Catal 6 (2016) 2280–2286.

[22] Y.F. Jia, K.M. Thomas, Adsorption of cadmium ions on oxygen surface sites in activated carbon, Langmuir 16 (2000) 1114–1122.

[23] D.M. Nevskaia, E. Castillejos-Lopez, A. Guerrero-Ruiz, V. Muñoz, Effects of the surface chemistry of carbon materials on the adsorption of phenol–aniline mixtures from water, Carbon 42 (2004) 653–665.

[24] D. Hulicova-Jurcakova, M. Seredych, G.Q. Lu, T.J. Bandosz, Combined effect of nitrogen- and oxygen-containing functional groups of microporous activated carbon on its electrochemical performance in supercapacitors, Adv. Funct. Mater. 19 (2009) 438–447.

[25] E. Raymundo-Piñero, F. Leroux, F. Béguin, A high-performance carbon for supercapacitors obtained by carbonization of a seaweed biopolymer, Adv. Mater. 18 (2006) 1877–1882.

[26] B. Hasse, J. Gläsel, A.M. Kern, D. Murzin, B.J.M. Etzold, Preparation of carbide-derived carbon supported platinum catalysts, Catal. Today 249 (2015) 30–37.

[27] I. Suarez-Martinez, C. Bittencourt, X. Ke, A. Felten, J.J. Pireaux, J. Ghijsen, et al., Probing the interaction between gold nanoparticles and oxygen functionalized carbon nanotubes, Carbon 47 (2009) 1549–1554.

[28] P. Yan, X. Zhang, F. Herold, F. Li, X. Dai, T. Cao, et al., Methanol oxidative dehydrogenation and dehydration on carbon nanotubes, Catal. Sci. Technol. 10 (2020) 4952–4959.

[29] F. Li, P. Yan, F. Herold, A. Drochner, H. Wang, T. Cao, et al., Oxygen assisted butanol conversion on bifunctional carbon nanotube catalysts, Carbon 170 (2020) 580–588.

[30] J. Zhang, X. Liu, R. Blume, A. Zhang, R. Schlögl, D.S. Su, Surface-modified carbon nanotubes catalyze oxidative dehydrogenation of n-butane, Science 322 (2008) 73–77.

[31] W. Qi, W. Liu, X. Guo, R. Schlögl, D. Su, Oxidative dehydrogenation on nanocarbon: intrinsic catalytic activity and structure-function relationships, Angew. Chem. Int. Ed. 54 (2015) 13682–13685.

[32] B.J. Meldrum, C.H. Rochester, In situ infrared study of the modification of the surface of activated carbon by ammonia, water and hydrogen, Faraday Trans 86 (1990) 1881–1884.

[33] B.J. Meldrum, C.H. Rochester, In situ infrared study of the surface oxidation of activated carbon in oxygen and carbon dioxide, Faraday Trans 86 (1990) 861–865.

[34] H. Boehm, Surface oxides on carbon and their analysis, Carbon 40 (2002) 145–149.

[35] S. Kohl, A. Drochner, H. Vogel, Quantification of oxygen surface groups on carbon materials via diffuse reflectance FT-IR spectroscopy and temperature programmed desorption, Catal. Today 150 (2010) 67–70.

[36] C. Moreno-Castilla, M.A. Ferro-Garcia, J.P. Joly, I. Bautista-Toledo, F. Carrasco–Marin, J. Rivera-Utrilla, Activated carbon surface modifications by nitric acid, hydrogen peroxide, and ammonium peroxydisulfate treatments, Langmuir 11 (1995) 4386–4392.

[37] M. Starsinic, R.L. Taylor, P.L. Walker, P.C. Painter, FTIR studies of Saran chars, Carbon 21 (1983) 69–74.

[38] J. Zawadzki, IR spectroscopy investigations of acidic character of carbonaceous films oxidized with HNO3 solution, Carbon 19 (1981) 19–25.

[39] M. Domingo-García, F.J. López-Garzón, M. Pérez-Mendoza, Effect of some oxidation treatments on the textural characteristics and surface chemical nature of an activated carbon, J. Colloid Interface Sci. 222 (2000) 233–240.

[40] J.S. Mattson, H.B. Mark, Infrared internal reflectance spectroscopic determination of surface functional groups on carbon, J. Colloid Interface Sci. 31 (1969) 131–144.

[41] J.M. Bakker, L. Mac Aleese, G. von Helden, G. Meijer, The infrared absorption spectrum of the gas phase neutral benzoic acid monomer and dimer, J. Chem. Phys. 119 (2003) 11180–11185.

[42] C. Ishizaki, I. Martí, Surface oxide structures on a commercial activated carbon, Carbon 19 (1981) 409–412.

[43] C. Moreno-Castilla, M. López-Ramón, F. Carrasco-Marín, Changes in surface chemistry of activated carbons by wet oxidation, Carbon 38 (2000) 1995–2001.

[44] P.E. Fanning, M. Vannice, A DRIFTS study of the formation of surface groups on carbon by oxidation, Carbon 31 (1993) 721–730.

[45] Q.-.L. Zhuang, T. Kyotani, A. Tomita, DRIFT and TK/TPD analyses of surface oxygen complexes formed during carbon gasification, Energy Fuels 8 (1994) 714–718.

[46] U.J. Kim, C.A. Furtado, X. Liu, G. Chen, P.C. Eklund, Raman and IR spectroscopy of chemically processed single-walled carbon nanotubes, J. Am. Chem. Soc. 127 (2005) 15437–15445.

[47] B.K. Pradhan, N.K. Sandle, Effect of different oxidizing agent treatments on the surface properties of activated carbons, Carbon 37 (1999) 1323–1332.

[48] F. Herold, O. Leubner, P. Pfeifer, D. Zakgeym, A. Drochner, W. Qi, et al., Synthesis strategies towards amorphous porous carbons with selective oxygen functionalization for the application as reference material, Carbon 171 (2021) 658–670.

[49] H.F. Gorgulho, J.P. Mesquita, F. Gonçalves, M.F.R. Pereira, J.L. Figueiredo, Characterization of the surface chemistry of carbon materials by potentiometric titrations and temperature-programmed desorption, Carbon 46 (2008) 1544–1555.

[50] J. Figueiredo, M. Pereira, M. Freitas, J. Órfão, Modification of the surface chemistry of activated carbons, Carbon 37 (1999) 1379–1389.

[51] J.L. Figueiredo, M.F.R. Pereira, M.M.A. Freitas, J.J.M. Órfão, Characterization of Active Sites on Carbon Catalysts, Ind. Eng. Chem. Res. 46 (2007) 4110–4115.

[52] T.J. Bandosz, J. Jagiello, C. Contescu, J.A. Schwarz, Characterization of the surfaces of activated carbons in terms of their acidity constant distributions, Carbon 31 (1993) 1193–1202.

[53] J. Ackermann, A. Krueger, Highly sensitive and reproducible quantification of oxygenated surface groups on carbon nanomaterials, Carbon 163 (2020) 56–62.

[54] S. Kundu, Y. Wang, W. Xia, M. Muhler, Thermal Stability and Reducibility of Oxygen-Containing Functional Groups on Multiwalled Carbon Nanotube Surfaces, J. Phys. Chem. C 112 (2008) 16869–16878.

[55] P. Düngen, R. Schlögl, S. Heumann, Non-linear thermogravimetric mass spectrometry of carbon materials providing direct speciation separation of oxygen functional groups, Carbon 130 (2018) 614–622.

[56] K. Friedel Ortega, R. Arrigo, B. Frank, R. Schlögl, A. Trunschke, Acid–base properties of n-doped carbon nanotubes, Chem. Mater. 28 (2016) 6826–6839.

[57] J.L. Figueiredo, M.F.R. Pereira, The role of surface chemistry in catalysis with carbons, Catal. Today 150 (2010) 2–7.

[58] A.M. Silva, B.F. Machado, J.L. Figueiredo, J.L. Faria, Controlling the surface chemistry of carbon xerogels using HNO3-hydrothermal oxidation, Carbon 47 (2009) 1670–1679.

[59] V. Likodimos, T.A. Steriotis, S.K. Papageorgiou, G.E. Romanos, R.R. Marques, R.P. Rocha, J.L. Faria, M.F. Pereira, J.L. Figueiredo, A.M. Silva, P. Falaras, Controlled surface functionalization of multiwall carbon nanotubes by HNO3 hydrothermal oxidation, Carbon 69 (2014) 311–326.

[60] U. Zielke, K.J. Hüttinger, W.P. Hoffman, Surface-oxidized carbon fibers, Carbon 34 (1996) 983–998.

[61] G.W. Howe, M. Bielecki, R. Kluger, Base-catalyzed decarboxylation of mandelylthiamin, J. Am. Chem. Soc. 134 (2012) 20621–20623.

[62] S. Kundu, W. Xia, W. Busser, M. Becker, D.A. Schmidt, M. Havenith, M. Muhler, The formation of nitrogen-containing functional groups on carbon nanotube surfaces, Phys. Chem. Chem. Phys. 12 (2010) 4351–4359.

[63] P.R. Griffiths, J.A. de Haseth, Fourier Transform Infrared Spectrometry, 2nd Ed., Wiley-Interscience, Hoboken, N.J, 2007.